ELSEVIER

Thermochimica Acta 271 (1996) 127–140

thermochimica acta

Modulated temperature DSC measurements: the influence of the experimental conditions[1]

J.E.K. Schawe

Universität Ulm, Sektion für Kalorimetrie, D-89069 Ulm, Germany

Received 30 May 1995; accepted 9 June 1995

Abstract

The influence of the experimental conditions on the results by modulated temperature DSC (MT-DSC) are investigated. The factors considered are temperature amplitude, frequency, underlying heating rates and sample preparation. Based on theoretical considerations and experimental results, practical recommendations are developed.

Keywords: Modulated temperature DSC; Glass transition; Cold crystallization; Melting; Experimental conditions

1. Introduction

It has now been 2 years since the first commercial modulated temperature DSC was introduced [1]. This calorimeter is based on a conventional heat flux DSC but with a sinusoidal temperature oscillation superimposed on the normal temperature program. The measured temperature difference between sample and reference can be calibrated as heat flow rate into the sample [2]. Reading proposed a method of evaluation of the raw data curve by separating a "reversing" and a "non-reversing" component of heat flow rate [3]. The "reversing component" is evaluated from the periodic part of the heat flow. The "non-reversing" component is the difference between the underlying heat flow (static heat flow) and the "reversing component". The static heat flow is evaluated by an averaging method (for example Fourier transformation and filtering). An alternative evaluation method has been reported based on the linear response approach [4]. From this approach, the static heat capacity c_β, and the complex heat capacity c^*, where

$$c^* = c' - ic'' \tag{1}$$

[1] Presented at the 11th Ulm Conference, Freiberg, Germany, 29–31 March, 1995.

SSDI 0040-6031 (95) 02562-6

result. The real part c' is the storage heat capacity (associated with mobility). The loss heat capacity c'' (associated with dissipation) is the imaginary part of c^*. The separation of the "reversing" component is identical with the modulus of c^*

$$|c| = \sqrt{c'^2 + c''^2} \tag{2}$$

The differences between both evaluation methods have been discussed [5]. The complex heat capacity can be converted into the "reversing" and "non-reversing" components; the reverse is not possible.

Recently the MT-DSC technique has been used with power compensated DSC [6], and with non sinusoidal temperature modulation [7,8]. With either technique it has been shown that MT-DSC is a good tool to separate different processes [9] and to measure the heat capacity with a height precision [10]. An advantage of the linear response approach is the capability to measure relaxation behaviour as a function of frequency [8].

Using a conventional DSC, the measuring result is known to be influenced by sample mass, thermal contact and scanning rate. These conditions have a greater effect on MT-DSC. In addition the frequency ν and the temperature amplitude T_a have an influence on the results [11]. An initial investigation by Sauerbrunn et al. [12–14] pointed to the importance of understanding these conditions. In this paper the investigation is broadened using a somewhat different approach. Namely the connection between the theoretical assumptions of the evaluation method and the experimental conditions are investigated.

2. Theory of the evaluation

The theory of the linear response approach has been described [4]. In the case of time dependent processes we can write the specific heat capacity as a function of time. The connection between the measured heat flow rate $\Phi(t)$ and the temperature change $\beta = dT/dt$ is given by

$$\Phi(t) = m\int_0^t \dot{c}(t-t')\beta(t')\,dt + \phi_0(T) \tag{3}$$

where m is the sample mass and $\dot{c} = dc/dt$.

In the case of a MT-DSC the temperature change β is the sum of the temperature program of a conventional DSC and the periodical term. The general formulation of the temperature $T(t)$ is

$$T(t) = T_0 + \beta_0 t + T_a \sum_{k=1}^{\infty} a_k \sin(k\omega_0 t) \tag{4}$$

where T_0 is the initial temperature, β_0 the underlying scanning rate, T_a the temperature amplitude of the periodical signal, a_k a factor and $\omega_0 = 2\pi\nu_0 = 2\pi/t_p$ (ν_0 is the frequency of the periodical signal and t_p the period time.)

If a sinusoidal temperature modulation is selected, Eq. (4) is

$$T(t) = T_0 + \beta_0 t + T_a \sin(\omega_0 t) \tag{5}$$

An alternative temperature modulation is a stepwise linear function (a succession of linear heating and cooling steps). The temperature function is then

$$T(t) = T_0 + \beta_0 t + \frac{4}{\pi} T_a \left(\frac{\sin(\omega_0 t)}{1} - \frac{\sin(3\omega_0 t)}{9} + \frac{\sin(5\omega_0 t)}{25} - \cdots \right) \tag{6}$$

In principle any periodic temperature function can be used but the quality of the measuring result is better when the relation between the first harmonic and the higher harmonics is large. The sinusoidal and the stepwise linear temperature programs are shown in Fig. 1.

Taking the derivative of the temperature (for example Eq. (4)) and inserting it into Eq. (3) we obtain the measured heat flow rate

$$\Phi(t, T) = m c_\beta(T) \beta_0 + m T_a \omega_0 \sum_{k=1}^{\infty} a_k k \left| c(k\omega_0, T) \right| \cos(k\omega_0 t - \varphi_k) \tag{7}$$

where c_β is the specific heat capacity which is dependent on the underlying heating rate, $|c|$ is the modulus of the complex heat capacity c^* and φ_k the phase lag between temperature change and heat flow rate.

The first term in Eq. (7) is similar to the conventional DSC curve Φ_c. The second term describes the periodic component of heat flow Φ_p. By averaging, both components can be obtained from the raw heat flow curve. If a non-sinusoidal temperature change is used, the Fourier analysis yields the first harmonic of the periodic component

$$\Phi_p(t, T) = m T_a \omega_0 a_1 \left| c(\omega_0, T) \right| \cos(\omega_0 t - \varphi) \tag{8}$$

The complex heat capacity is given by amplitude and phase lag

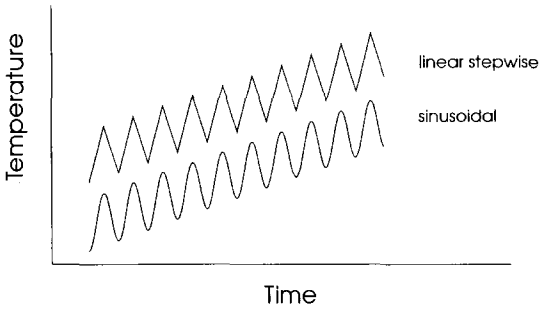

Fig. 1. Different dynamic temperature programs.

$$c'(\omega_0) = |c(\omega_0)| \cos(\varphi) \tag{9}$$

$$c''(\omega_0) = |c(\omega_0)| \sin(\varphi) \tag{10}$$

Eq. (7) is only valid on the condition that the underlying scanning rate is low. This means the change of the heat capacity during one period is low (quasi isothermal conditions during one period). This is a fundamental condition for every separation method.

3. Experimental

The measurements were carried out on a modified Perkin Elmer DSC 7. In this special calorimeter the program temperature is modulated with a sinusoidal or a linear stepwise temperature change. The frequency can be selected between 200 and 1 mHz. The range of the amplitude is from 0.1 to 10 K. The DSC 7 is a power compensated DSC. The measurement principle is described in thermal analysis textbooks [15]. In addition to the usual DSC outputs the average temperature between sample and reference furnace is measured. With the help of this temperature and the heat flow signal the storage and loss heat capacity (c' and c'') are calculated by Fourier analysis from the periodic component.

For the case of a linear stepwise temperature modulation the program and the sensor temperature, as well as their first harmonic, are shown in Fig. 2. The dynamic component of measured heat flow rate and its first harmonic are shown in Fig. 3. The correspondence between the sensor and program temperature is very good. For these evaluation only the first harmonics of the sensor temperature and the heat flow rate are used.

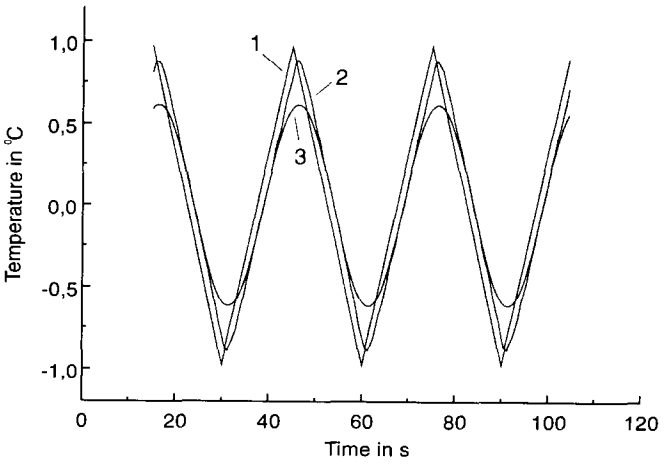

Fig. 2. Program temperature, sample temperature and first harmonic of the sample temperature in the case of a linear stepwise temperature modulation (amplitude approximately 1 K, frequency: 33 mHz); 1, program temperature; 2, sensor temperature; 3, first harmonic of sensor temperature.

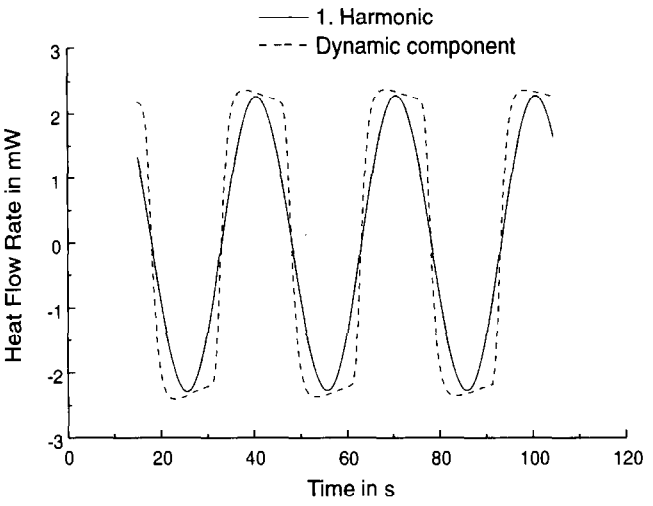

Fig. 3. Dynamic component of measured heat flow rate and its first harmonics at the temperature program as in Fig. 2.

The separation of the periodic and the underlying component is carried out through averaging. The underlying component yields c_β. The calibration procedure of the periodical component will be described elsewhere [11].

The samples were commercial poly(ethylene-therephthalate) (PET) and polystyrene (PS). The sample mass, temperature amplitude, frequency, the underlying heating rate and the wave form of the periodic signal were varied. Unless otherwise noted the sinusoidal temperature modulation was used.

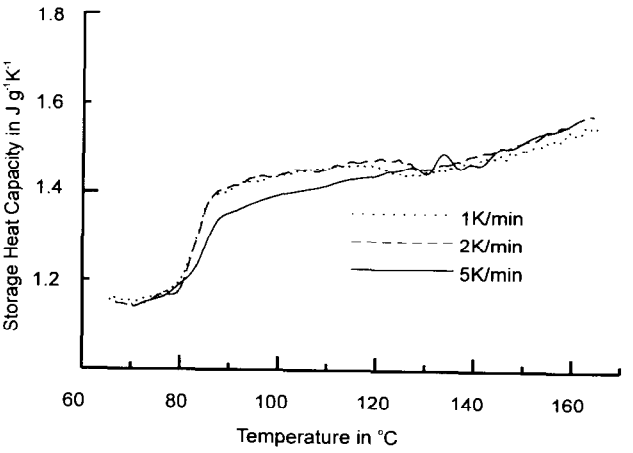

Fig. 4. Storage heat capacity of PET in the glass transition and the cold crystallization regions measured at different underlying heating rates (sample mass 4.324 mg, frequency 42 mHz, temperature amplitude 0.2 K).

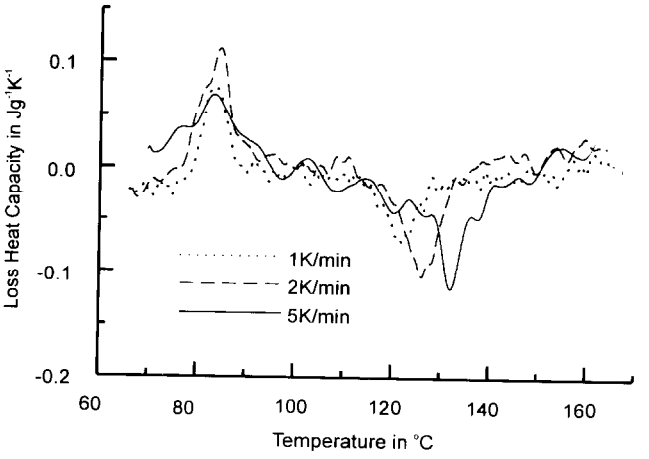

Fig. 5. Loss heat capacity of PET (same conditions as in Fig. 4).

4. Results and discussion

In the case of conventional DSC the main parameters used to describe an experiment are the start and the end temperature and the scanning rate β_0. To describe an MT-DSC experiment we need additional parameters, namely the amplitude and frequency. The mathematical procedures for evaluation and the linear response theory required a quasi constant underlying temperature and a small temperature amplitude. On the other hand a relatively large scanning rate leads to a short time of experiment, and a large temperature amplitude yields a good signal to noise ratio for the complex heat capacity. In order to find the optimum conditions we investigated the influence of the different experimental parameters on the measuring results.

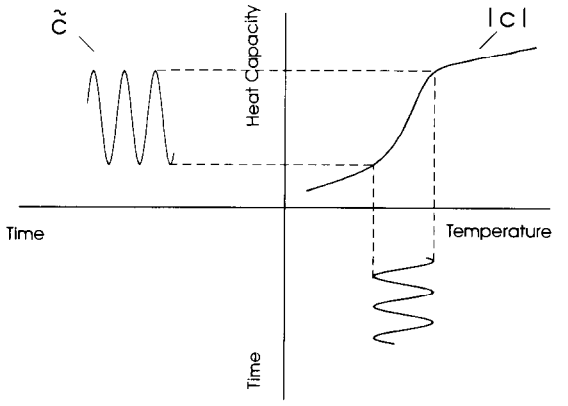

Fig. 6. Scheme to illustrate the construction of the temperature and time dependent dynamic change of the heat capacity.

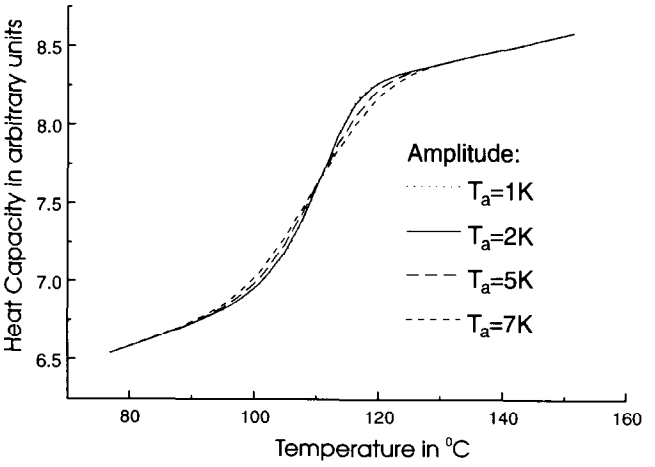

Fig. 7. Storage heat capacity, calculated from the simulated curves at different amplitudes.

4.1. Variation of the underlying heating rate

The underlying scanning rate is restricted by the experimental conditions. On the one hand, normally the time of a run should be as short as possible. On the other hand, the assumption of the numerical evaluation of the raw data is that of quasi isothermal conditions. This means that the temperature change is show and the change of the heat capacity during one period is relative small. As a result the maximum heating rate depends on

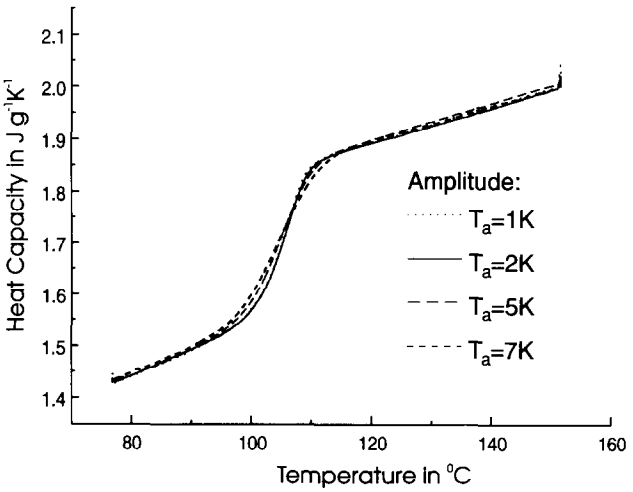

Fig. 8. Storage heat capacity of polystyrene in the glass transition region measured at different amplitudes (sample mass 4.230 mg, underlying cooling rate 1 K min^{-1}, frequency 36 mHz).

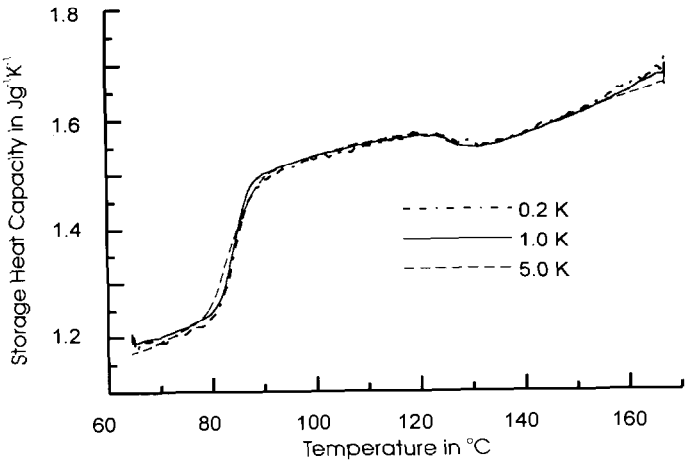

Fig. 9. Storage heat capacity of PET in the glass transition and the cold crystallization regions measured at different temperature amplitude (sample mass 4.324 mg, frequency 42 mHz, $\beta_0 = 2$ K min^{-1}).

the dynamic requirement of the thermal event. In the case of the glass transition and cold crystallization of PET one can use a change in the underlying temperature of approximately 0.5 K per period. In the melting region this rate is lower (e.g. 0.3 K per period). This effect is illustrated in Figs. 4 and 5. It is well known that the cold crystallization temperature is dependent on the heating rate while the dynamic glass transition is independent of it [4,8]. The figures show the effect of the underlying heating rate on the temperature of the step in the storage heat capacity which occurs during crystallization. The temperature shift of the maxima of crystallization is the same. In this case the underlying

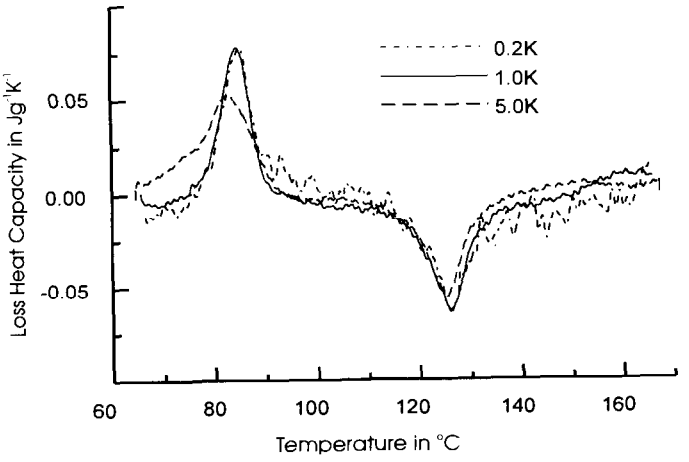

Fig. 10. Loss heat capacity of PET (same conditions as in Fig. 9).

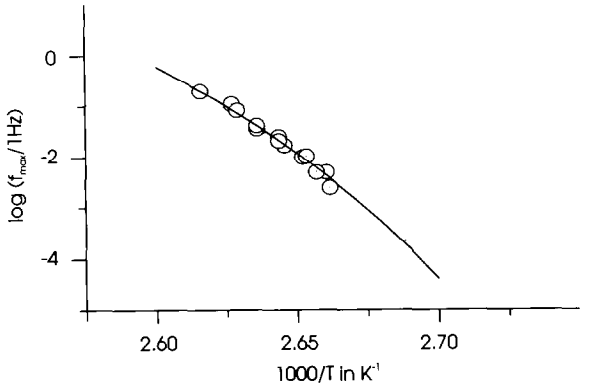

Fig. 11. Activation diagram of the dynamic thermal glass transition of PS.

heating rates are 1 and 2 K min^{-1} (or approximately 0.4 and 0.8 K increment per period). At larger heating rate (5 K min^{-1} or 2 K increment per period) the experimental result is wrong (especially in the storage heat capacity). By using of lower frequencies the maximal heating rate decreased.

4.2. Variation of the temperature amplitude

The temperature amplitude is limited by heat transfer into the furnaces and the sample, as well as by the magnitude of the thermal event. The first influence has been described in the case of a heat flux DSC [12]. In a power compensated DSC the situation is differ-

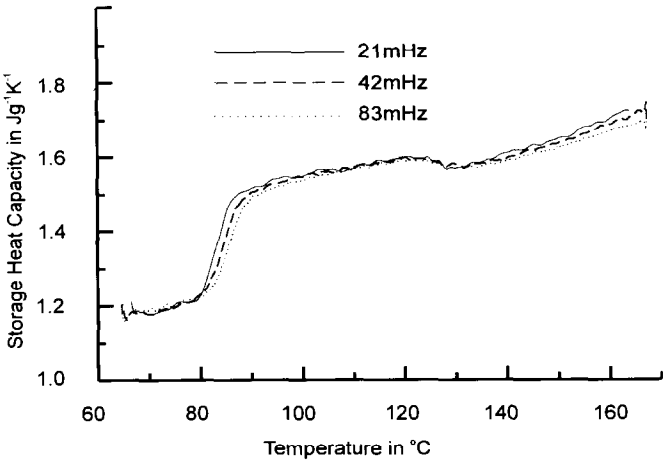

Fig. 12. Storage heat capacity of PET in the glass transition and the cold crystallization region measured at different frequencies (sample mass 4.324 mg, temperature amplitude 42 mHz, underlying heating rate 2 K min^{-1}).

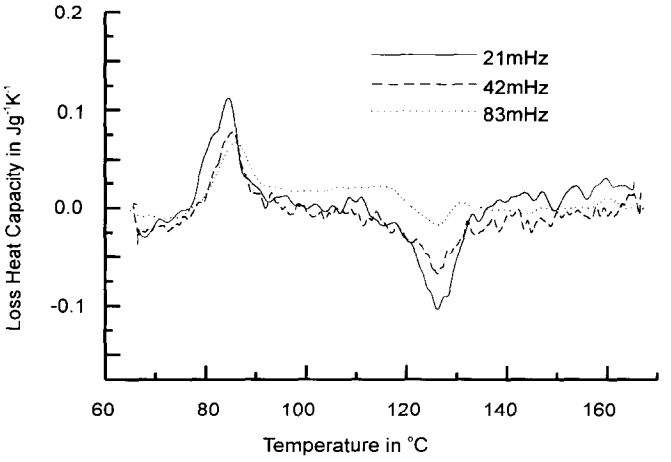

Fig. 13. Loss heat capacity of PET (same conditions as in Fig. 12).

ent because the measured temperature directly influences the power of the heater. Hence the temperature amplitude of the sample is the same as that of the program temperature over a wide frequency range. Only at relatively high frequencies is the sample temperature decreased, thus necessitating careful calibration [11].

The specific heat capacity is calculated from the amplitude of the measured heat flow rate (see Eq. (8)). Ideally this requires that the heat capacity be constant over one period.

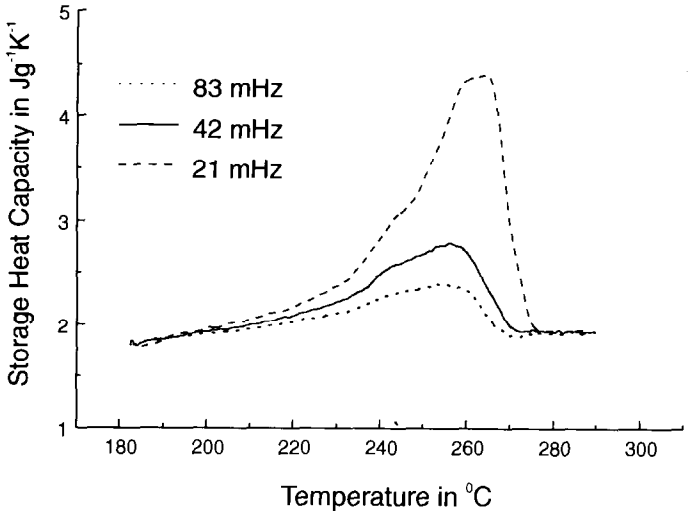

Fig. 14. Storage heat capacity of PET in the melting region measured at different frequencies (sample mass 4.324 mg, amplitude 0.2 K, underlying heating rate 1 K min^{-1}).

This requirement is satisfied when the change of heat capacity is low in the temperature interval $[T_0 - T_a, T_0 + T_a]$. If this condition is not satisfied the results may be in error. In order to investigate this influence of the amplitude on the measured signal we have simulated the measured curves for the case of the glass transition of polystyrene. Here Eq. (8) is changed to

$$\Phi_p(t,T) = mT_a\omega_0 a_1 \tilde{c}(T,t) \tag{11}$$

where $\tilde{c}$ includes the change in temperature and time as given by

$$\tilde{c}(T,t) = |c(\omega_0,T)| \cos(\omega_0,t) \tag{12}$$

The construction of $\tilde{c}$ is illustrated in Fig. 6.

This simulated curve is used as input function in the evaluation program. The temperature amplitude is varied between 1 and 7 K. The result is shown in Fig. 7. For the amplitudes of 1 and 2 K we get nearly the same result. Broader heat capacity steps are the result of using of larger amplitudes. These larger amplitudes adversely effect the quality of the data. By comparison, in Fig. 8, the experimental results using the same conditions are shown. The simulated and measured curve shapes are similar.

The storage and loss heat capacity of poly(ethylene therephthalate) in the glass transition and cold crystallization region are shown in Figs. 9 and 10. Lower amplitudes (0.2 and 1 K) yield the same curve shape. However, the ratio of signal to noise is better with increase of the amplitude. Only at an amplitude of 5 K is the shape of the resulting curves influenced. This effect is especially significant for the loss of heat capacity.

In summary, the maximum amplitude which should be used is dependent on the rate

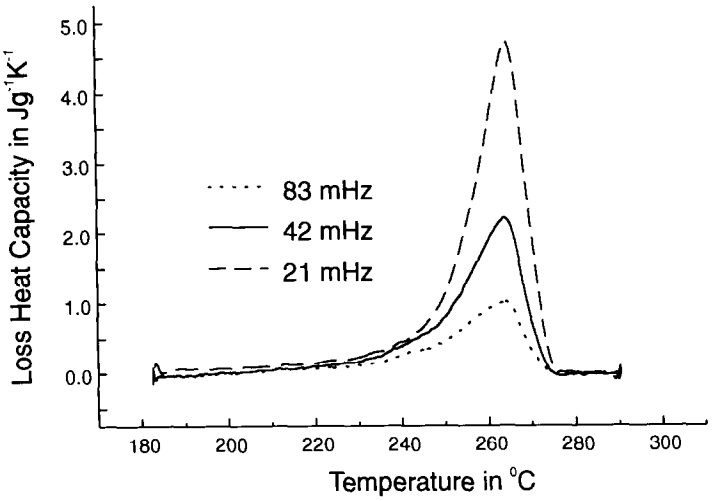

Fig. 15. Loss heat capacity of PET (same conditions as in Fig. 14).

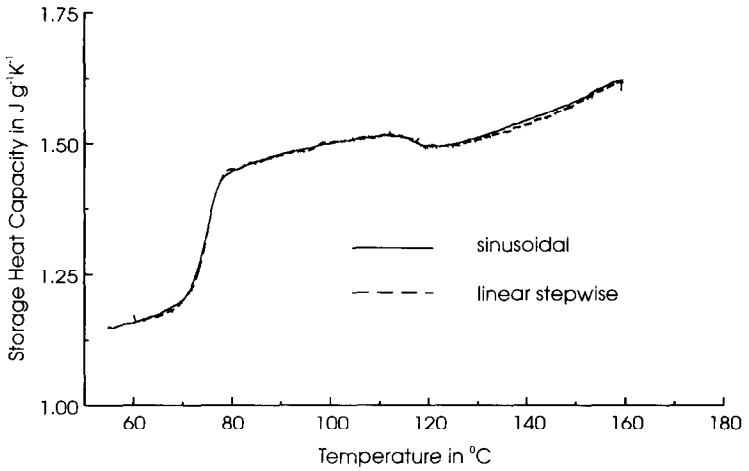

Fig. 16. Storage heat capacity of PET in the glass transition and the cold crystallization regions measured at different modulated signal forms (sample mass 4.324 mg, frequency 33 mHz, amplitude 0.8 K, underlying heating rate 1 K min^{-1}).

of heat capacity change. In the case of glass transition and cold crystallization it is possible to use temperature amplitudes of more than 1 K. The dynamic change of the signal in the melting region is much larger. The useful maximum amplitude should be not larger than 0.2 K.

4.3. Variation of the frequency

In Ref. [14] the effect of the period (or frequency) is discussed only in relationship to its influence on the calibration. This calibration is very important for MT-DSC, but moreover, if the instrument is calibrated [11], the sample well prepared and the amplitude and underlying rate are optimized (see above), the frequency dependence of the data gives additional information about the thermal event. Without detailed discussion we offer three examples.

The first is the glass transition of polystyrene. We define the dynamic glass transition temperature as the maximum temperature of the loss heat capacity peak. In short, the glass transition temperature T_g is dependent on the frequency. If the frequency is increased then T_g is also increased. In the activation diagram (Fig. 11) we observe a concave curve. This is typical for cooperative phenomena.

The second example is the cold crystallization of PET. The storage heat capacity shows a decrease, and the loss of heat capacity an exothermic peak. This behaviour is independent of frequency and reflects the change of the molecular motion in the amorphous phase during the crystallization (see Figs. 12 and 13).

The last example is the melting of PET (Figs. 14 and 15). Before the measurement all samples are crystallized at 170°C for 30 min. Afterwards the sample is measured at an underlying heating rate of 1 K min^{-1} and an amplitude of 0.2 K. The height of the peak depends on the frequency. The maximum temperature of the storage peak is less than that

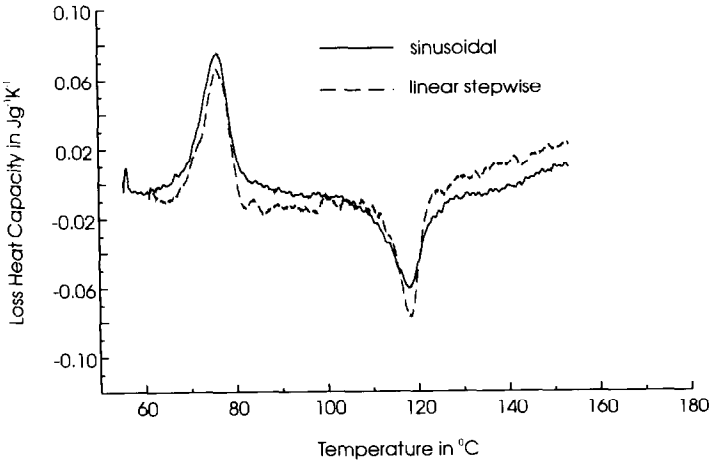

Fig. 17. Loss heat capacity of PET(same conditions as in Fig. 16).

of the loss of heat capacity. The storage component maximum temperature increases with increased frequency. This is in contrast to the peak maximum of the losses signal which is relatively temperature independent.

For a detailed interpretation of these examples, see elsewhere (e.g. [8,16,17]).

4.4. The influence of other conditions

Other conditions in this context are the signal form (sinusoidal or linear stepwise modulation), sample preparation and sample pans.

A comparison of the complex heat capacity measured at different modulations (dynamic component is a sinusoidal or the linear stepwise function) is shown in Figs. 16 and 17. These figures show no significant difference between signal forms.

The best experimental results are obtained when a thin film is used and the contact between sample and sample pan is good. For a typical polymer up to frequencies of approximate 7 mHz the sample mass should not be higher than 5 mg, and the contact area between sample pan and furnace should be large and homogenous.

The influence of the sample pan on the measurement result is minimized if the mass in all cases (sample and base line run) are the same. For best results the pan mass should be as small as possible.

5. Conclusions

One large problem by MT-DSC measurements is the reproducibility of the results. A meaningful measurement is only possible when the conditions (e.g. amplitude, frequency, underlying scanning rate and sample preparation) are well selected. The optimal conditions are dependent on the kind of thermal event. For example, in the case of a glass

transition, a practical temperature amplitude is 1.5 K, and the change of the underlying temperature of approximately 0.7 K per period is appropriate. In the melting region these values should be lower (about $T_a = 0.2$ K and the change of the underlying temperature 0.2 K per period). The important condition for the choice of the underlying heating rate is the change of the heat capacity during a period. The maximal temperature amplitude is limited by the heat capacity change over one period. The experimental results show that the related change of the heat capacity per period should be less than 0.6 mJ K^{-1}.

For certain types of investigation it is necessary to carefully plan the experiment. For example, the underlying heating rate should be constant when the frequency dependence of the melting behaviour is investigated. For the realization of this condition the width of the frequency range must be known and the maximum change of the underlying temperature per period should be considered.

The technique of MT-DSC is one which holds considerable scope to clarify the time dependent characteristics of polymers. However, it is a technique which requires much of the operator and instrument.

References

[1] P.S. Gill, S.R. Sauerbrunn and M. Reading, J. Thermal Anal., 40 (1993) 931.
[2] B. Wunderlich, Y. Jin and A. Boller, Thermochim. Acta, 238 (1994) 277.
[3] M. Reading, D. Elliott and V.L. Hill, J. Thermal Anal., 40 (1993) 949.
[4] J.E.K. Schawe, Thermochim. Acta, in press.
[5] J.E.K. Schawe, Thermochim. Acta, 260 (1995) 1.
[6] B. Cassel and M. DiVito, 23rd NATAS Conf. Proc., Toronto, 1994, p. 411.
[7] R. Riesen and B. Perrenot, Proc. STK Meeting, Vabella, 1994.
[8] A. Hensel, J. Dobbertin, J.E.K. Schawe, A. Boller and C. Schick, J. Thermal Anal., submitted.
[9] W.J. Sichina, 23rd NATAS Conf. Proc., Toronto, 1994, p. 38.
[10] A. Boller, Y. Jin and B. Wunderlich, J. Thermal Anal., 42 (1994) 307.
[11] J.E.K. Schawe, M. Margulies and B. Cassel, unpublished.
[12] S.R. Sauerbrunn and R.L. Blaine 23rd NATAS Conf. Proc., Toronto, 1994, p. 57.
[13] S.R. Sauerbrunn and L.C. Thomas, 23rd NATAS Conf. Proc., Toronto, 1994, p. 45.
[14] S.R. Sauerbrunn, P.S. Gill and J.A. Foreman, 23rd NATAS Conf. Proc., Toronto, 1994, p. 51.
[15] W. Hemminger and G.W.H. Höhne, Calorimetry – Fundamentals and Practice, Verlag Chemie, Weinheim, 1984.
[16] J.E.K. Schawe and G.W.H. Höhne, J. Thermal Anal., submitted.
[17] J.E.K. Schawe, unpublished.